Atmospheric Research 262 (2021) 105804

Contents lists available at ScienceDirect

Atmospheric Research

journal homepage: www.elsevier.com/locate/atmosres

Opposite anomalous synoptic patterns for potential California large wildfire spread and extinguishing in 2018 cases

Weihong Qian [a,b,*], Yang Ai [b], Jin-Yi Yu [c], Jun Du [d]

[a] Institute of Tropical and Marine Meteorology/Guangdong Provincial Key Laboratory of Regional Numerical Weather Prediction, China Meteorological Administration, Guangzhou 510640, China
[b] Department of Atmospheric and Oceanic Sciences, Peking University, Beijing 100871, China
[c] Department of Earth System Science, School of Physical Sciences, University of California, Irvine, CA 92697-3100, USA
[d] Environmental Modeling Center, NCEP/NWS/NOAA, College Park, MD 20740, USA

ARTICLE INFO

Keywords:
Wildfire
Favorable fuel
Meteorological condition
Anomalous synoptic pattern

ABSTRACT

The consecutive occurrence of three large wildfires in 1 year is rarely seen in northern California including the deadliest case during 8–25 November 2018 in Butte County. They happened under favorable fuel and meteorological conditions including long-term warming trends, normal summer-autumn warm-dry climate, and extreme heated air masses with strong offshore wind. The former two meteorological conditions contribute a background for large wildfires but extreme heated air masses and strong offshore winds are critical potentials for a fire spread. The relationship between extreme heated/cooled air masses and the three large wildfires was carefully examined from their starts to extinguishing. An anomaly-based synoptic analysis method is used by separating atmospheric variables into climatology and anomalies. A 3-dimensional anomalous synoptic pattern of atmospheric variables is established for the three wildfire cases in 2018. The analysis showed that one anomalous warm-air mass in the mid-to-low troposphere dynamically associated with a positive center of geopotential height (GPH) anomalies at the upper troposphere (150–300 hPa) is an anomalous synoptic pattern indicating a potential large wildfire spread, and conversely by negative anomalies when the fires were extinguished. The ECMWF model seems to be capable of predicting such anomalous temperature-pressure patterns to indicate possible fire spread and extinguishing.

1. Introduction

Wildfires can threaten native ecosystems and human lives (Rager et al., 2021; Santos et al., 2021; Xiang et al., 2021). There are frequent and even some large wildfires in the western United States because of vast flammable chaparral scrub vegetation under warm-dry and strong offshore wind meteorological conditions. Wildfires often cause serious socioeconomic destruction and significant loss of life (Abatzoglou and Williams, 2016; Crockett and Westerling, 2018; Dennison et al., 2014; Mass and Ovens, 2019; Williams et al., 2019). In northern California, North Coast and the Sierra Nevada are largely covered by forests, where fuel condition is favorable for large wildfires under suitable meteorological conditions. Fires in California are known to be exacerbated by warm-dry conditions with strong downslope winds (Goss et al., 2020; Khorshidi et al., 2020). For the temperature variation, it can be categorized into three components based on their timescales: the long-term global warming trend, medium-term annual or seasonal warm-dry cycle, and short-term individual heated/cooled weather extremes. Thus, the first question is how these temperature variations in different timescales impact large fire events.

The relationship between long-term increased fires and the warm-dry trend is widely mentioned (Goss et al., 2020; Swain, 2021). Williams et al. (2019) found that California wildfires experienced a fivefold increase in the annual burned area, mainly due to more than an eightfold increase in summer forest fire extent from 1972 to 2018. They concluded that the increased summer forest-fire area very likely occurred due to the increased atmospheric aridity which was caused by the warming trend. Since the early 1970s the warm-season days have been warmed by approximately 1.4 °C. Similar trend results are also reported by other studies. For example, the annual burned area is increased substantially

* Corresponding author at: Institute of Tropical and Marine Meteorology/Guangdong Provincial Key Laboratory of Regional Numerical Weather Prediction, China Meteorological Administration, Guangzhou 510640, China.
E-mail address: qianwh@pku.edu.cn (W. Qian).

https://doi.org/10.1016/j.atmosres.2021.105804
Received 20 June 2021; Received in revised form 5 August 2021; Accepted 6 August 2021
Available online 8 August 2021

in recent decades due to the increased frequency and size of large wildfires (Abatzoglou and Williams, 2016; Balch et al., 2018; Dennison et al., 2014). This long-term trend of increasing burned area has reached a top stage in 2017 and 2018 by particularly extreme wildfire activity with substantial loss of life and property. In 2017, the largest individual wildfire was the Thomas Fire, while most structures were destroyed by the Tubbs Fire. The Tubbs Fire also led to 22 fatalities (Mass and Ovens, 2019). In 2018, the largest individual wildfire is the Mendocino Complex Fire and the deadliest wildfire led to 86 fatalities is the Camp Fire (Brewer and Clements, 2020; Silveira et al., 2021). Some studies mentioned that the human-caused warming has already significantly enhanced the trend of wildfire activity in California, particularly in the forests of the Sierra Nevada and North Coast (Abatzoglou and Williams, 2016; Keeley and Syphard, 2016; Williams et al., 2015, 2019).

Many studies of large wildfire focused on the summer-autumn warm-dry climate condition with an abundant fuel condition in the California region (Balch et al., 2017; Crockett and Westerling, 2018; Jin et al., 2015; Mao et al., 2015; Marlon et al., 2012; Miller et al., 2012; Robeson, 2015; Rundel, 2018; Syphard et al., 2007; Thorne et al., 2017; Westerling et al., 2011). Summer-autumn fire extent seasonally depends on air heat and atmospheric aridity that dries out fuel. As indicated by previous studies (Miller and Schlegel, 2006), wildfires in the California coastal region typically occur during the fall season prior to the winter rains. During this period of the season, an inland high pressure and an offshore low pressure often form a strong pressure gradient over California, resulting in heated air mass and high offshore winds with low humidity. A similar description can also be noted from other studies (Guzman-Morales et al., 2016; Moritz et al., 2010). This seasonal cycle of warm-dry climate in summer and dry-wind climate in autumn explains why wildfire spreads in summer and autumn faster than that in winter and spring.

Except for the long-term global-warming induced increase trend and the seasonal cycle of a high frequency of large wildfires occurred in summer and autumn, large wildfires could also happen in an off-peak season when short-term individual weather extreme (such as heated air mass and high offshore winds) occurs. A few of them could even become severe. For example, the large Thomas Fire was spread in winter (4 December 2017 to 12 January 2018). In some cases, the intensity of short-term weather extreme can largely exceed long-term global warming trend and medium-term summer-autumn warm climate conditions for drying air and forcing fire. As indicated by Minnich and Chou (1997), the reality is that suppression of very large fires was never effective, meaning that suppression forces cannot control large fires. These large fires are directly associated with strong offshore winds (Jin et al., 2014; Kolden and Abatzoglou, 2018), persistent heat and dry weather conditions (Bendix and Hartnett, 2018). The strong winds for fire spread are known locally as Santa Ana winds in southern California and Diablo winds in northern California., These winds are more generally referred to as foehns, namely dry-heat offshore winds, or the meteorological term “downslope winds” (Billmire et al., 2014; Guzman-Morales et al., 2016; Hughes and Hall, 2010; Moritz et al., 2010). For the application to real-world fire weather forecasting, the long-term warming trend can be expected for future several years and the medium-term dry warm climate is a well-known and repeated seasonal cycle. Therefore our second question is how to identify the spatiotemporal structure of short-term weather extremes for the description of each large fire length, which will be the main focus of this study.

Many works focused on the study of started fire weather conditions such as dry-heat offshore wind and surface pressure field but few concerned the ended fire weather condition from spatial synoptic analyses. To capture short-term weather extreme signals for what a large fire starts and ends, we will apply an anomaly-based analysis method to fire weather study. Specifically, we will compare the difference of synoptic patterns based on total and anomalous synoptic analyses for their spread and extinguishing of three California wildfires in 2018. The purpose of this study is not to discover new atmospheric circulations associated with fire weather but introduces a new angle (anomaly approach) to look at those atmospheric conditions differently and more completely. Although anomaly is used in the meteorology community, the way we show in this study is different from those traditional approaches. In a traditional method, 2-dimensional relative increments, e.g., warmer temperature, drier air, and stronger wind (compared to a reference or climatology) at a fixed level or levels (e.g., near the surface) are often used as favorable conditions for fire weather prediction. However, this study describes a 3-dimensional anomalous structure or pattern throughout the entire atmosphere, which has not yet been explored in fire weather research and operations so far. We are hoping that this study will provide a new insight or thinking for developing innovative tools for fire weather prediction in the future. Furthermore, the ECMWF model products are used to demonstrate if current numerical weather prediction (NWP) models have the ability to predict the 3-dimensional anomalous atmospheric structure revealed by this study related to wildfire spread and extinguishing. After this introduction, datasets and approaches are presented in Section 2. The three large wildfires are described in Section 3. General evolutions of vertical structures of anomalous variables are given in Section 4. Anomalous synoptic patterns before fire spread and extinguishing are compared for the first two cases in Section 5 and confirmed for the third case in Section 6. Summary and discuusion are given in Section 7.

2. Datasets and anomaly-based analysis approach

2.1. Datasets

To identify anomalous synoptic patterns related to California large wildfires, four datasets are used in this study. The first dataset is a global atmospheric reanalysis dataset, the ERA-Interim (Dee et al., 2011), from the European Centre for Medium-Range Weather Forecasts (ECMWF). Geopotential height (GPH), air temperature, and horizontal winds at the pressure levels from 1000 hPa to 50 hPa with the horizontal resolution of $0.75^\circ \times 0.75^\circ$ are obtained from the ECMWF's website (https://apps.ecmwf.int/datasets/data/interim-full-daily/levtype=sfc/). This data is used to compare the different patterns extracted from total and anomalous synoptic analyses.

The second dataset used is the product of the ensemble prediction systems (EPS) at the ECMWF, obtained from “The International Grand Global Ensemble” project (TIGGE, http://apps.ecmwf.int/datasets/data/tigge/levtype=pl/type=cf/). This study used the 10-day (240 h) ECMWF EPS forecasts of GPH and temperature at 8 levels from 1000 hPa to 200 hPa with the horizontal resolution of $0.75^\circ \times 0.75^\circ$, based on 51 ensemble members. The ensemble mean of the 51 members is used to examine whether anomalous synoptic patterns associated with fire weather condition could be accurately predicted by this medium-range NWP model.

The third dataset is the daily global historical climatology network dataset (GHCN-Daily), Version 3.25 (Menne, 2012a, Menne et al., 2012b), including observed daily maximum/minimum surface air temperatures and precipitations in California from the National Climatic Data Center of the National Oceanic and Atmospheric Administration (NOAA). The data of five stations, near where the fires happened, is used to reflect the information of dry/wet and hot/cold weather.

The fourth dataset is the fire statistics and the data of news releases about the incident from the California Department of Forestry and Fire Protection (CAL FIRE) website (http://www.fire.ca.gov/). This study uses data of the Top 20 largest California wildfires and the incident facts since 1932 but the CAL FIRE dataset only provided 4 cases of the daily active fire area and burned area in 2017 and 2018.

2.2. Anomaly-based analysis approach

The anomaly-based analysis approach (Eq. 1) separates climatic variable $\widetilde{v}_d(\lambda, \varphi, p, t)$ and anomalous component $v'_{(d,y)}(\lambda, \varphi, p, t)$ from a

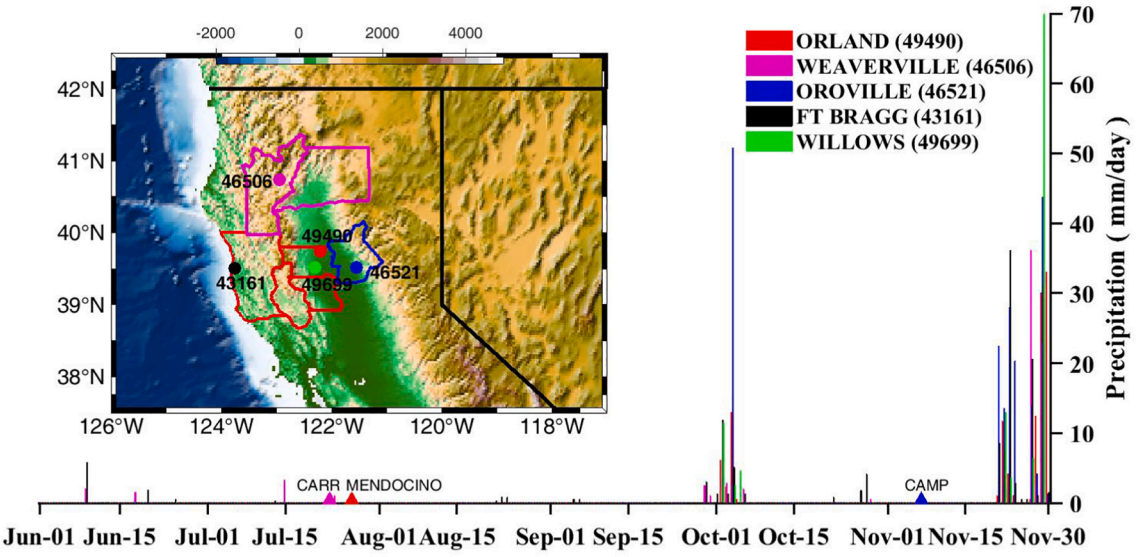

Fig. 1. Three California wildfires burned: 1) CARR fire, from 23 July to 30 August 2018 in Shasta County and Trinity County (magenta area, north part); 2) MENDOCINO COMPLEX (or MENDOCINO for simplicity) fire, from 27 July to 18 September 2018 in Mendocino County, Glenn County, Colusa County and Lake County (red area, south part); and 3) CAMP fire, from 8 to 25 November 2018 in Butte County (blue area, central east part) with daily precipitation (bar chart, mm/day in the y-axis) at five observational stations from 1 June to 30 November 2018 in the x-axis. Three triangles indicate started dates of the three fires. (For interpretation of the references to color in this figure legend, the reader is referred to the web version of this article.)

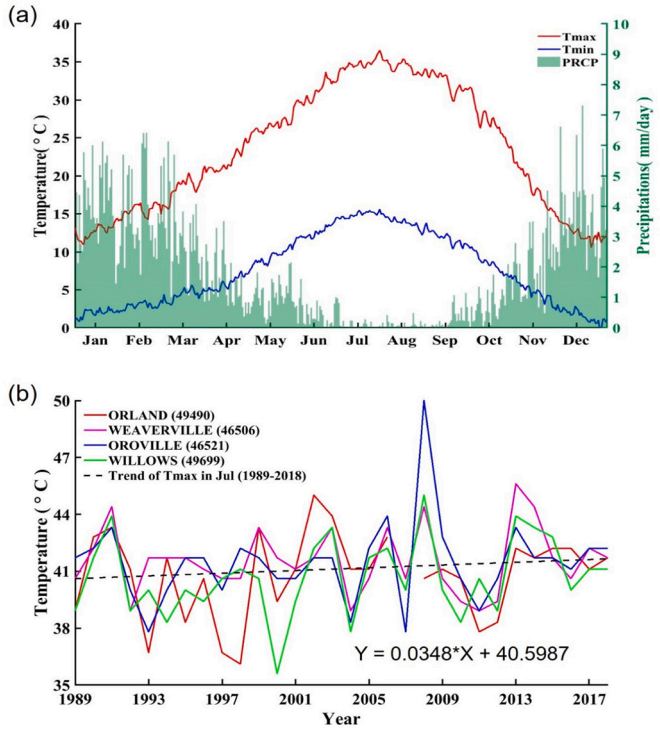

Fig. 2. (a) The daily climate averaged for the 1989–2018 period of maximum temperature (Tmax, ^{O}C in red line) and minimum temperature (Tmin, ^{O}C in blue line, left y-axis) as well as precipitation (PRCP, mm/day, right y-axis) based on the data of observational stations same as in Fig. 1 but without the coastal station of NO. 43161 (FT BRAGG). (b) The temperature series (^{O}C in color lines, y-axis) of monthly-mean Tmax in July on the stations located in Fig. 1 and the long-term trend (black dashed line) of Tmax in July from 1989 to 2018. (For interpretation of the references to color in this figure legend, the reader is referred to the web version of this article.)

total field $v_{(d,y)}(\lambda,\varphi,p,t)$. This approach of decomposition has been proven to be useful in weather extremes (Qian et al., 2021b), mostly for tropical cyclones (Qian et al., 2014) and heavy rainfall (Qian et al., 2021a).

$$v_{(d,y)}(\lambda,\varphi,p,t) = \widetilde{v}_d(\lambda,\varphi,p,t) + v'_{(d,y)}(\lambda,\varphi,p,t) \quad (1)$$

where t represents time (24 h a day) on a calendar date d in a year y, while λ, φ and p denote longitude, latitude, and pressure level respectively.

Daily extreme weather events such as heat waves and cold surges are seen as results of anomalous synoptic-scale systems relative to climatology (Qian, 2017). The climatology of a certain location and a certain time is considered as a static state under the thermodynamic equilibrium of the earth-atmosphere system, which is only forced by the solar radiation (solar declination) and surface conditions rather than daily weather disturbances. The climatology is estimated by averaging the reanalysis data at time t on calendar date d over M years,

$$\widetilde{v}_d(\lambda,\varphi,p,t) = \sum_{y=1}^{M} v_{(d,y)}(\lambda,\varphi,p,t) \Big/ M \quad (2)$$

where y runs for M years ($M > 30$ years). It is assumed that the positive and negative anomalies of meteorological variables at a specific grid point and a given calendar time cancel each other during the M years. In the previous study (Qian et al., 2014), y runs from 1981 to 2010 for $M =$ 30 years. The ERA-Interim data of 4 times per day with 6-h intervals have been used to obtain the climatology globally. For anomalous synoptic analysis, both relative and normalized anomalies are used to study extreme weather events. For example, the synoptic analysis of normalized anomalies was initially used by Grumm and Hart (2001) and has now become a common tool in daily operation for short-range weather forecasts (Du et al., 2013; Graham and Grumm, 2010; Grumm, 2011; Hart and Grumm, 2001; Junker et al., 2009; Junker et al., 2008). Jiang et al. (2016) have a comparative study between the two forms of anomalies. Relative or raw anomaly will mainly be used in this study.

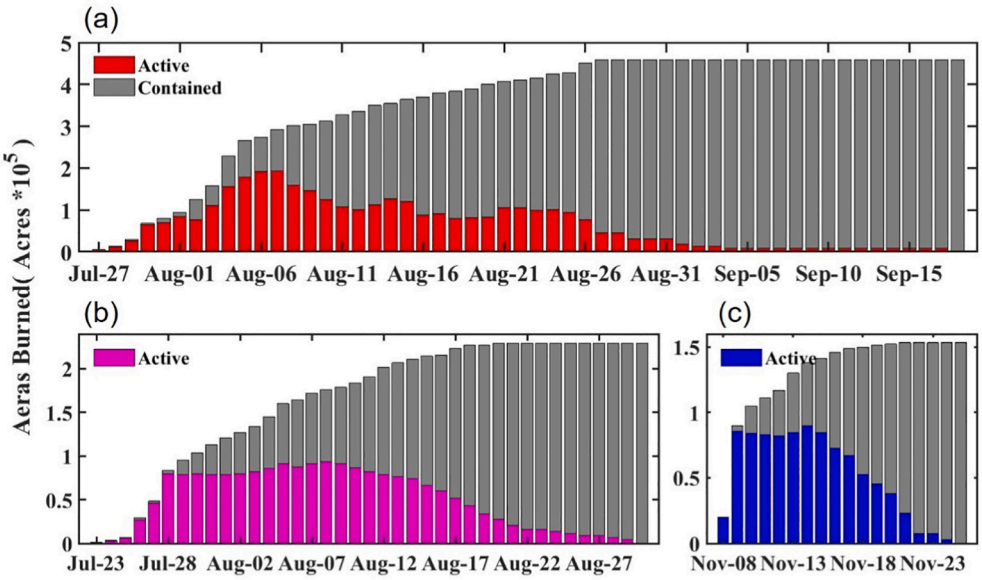

Fig. 3. Active fire area (color bar, Acres×10^5) and burned area (grey bar, Acres×10^5) in (a) the MENDOCINO COMPLEX Fire from 27 July to 18 September, (b) the CARR Fire from 23 July to 30 August, and (c) the CAMP Fire from 8 November to 25 November 2018.

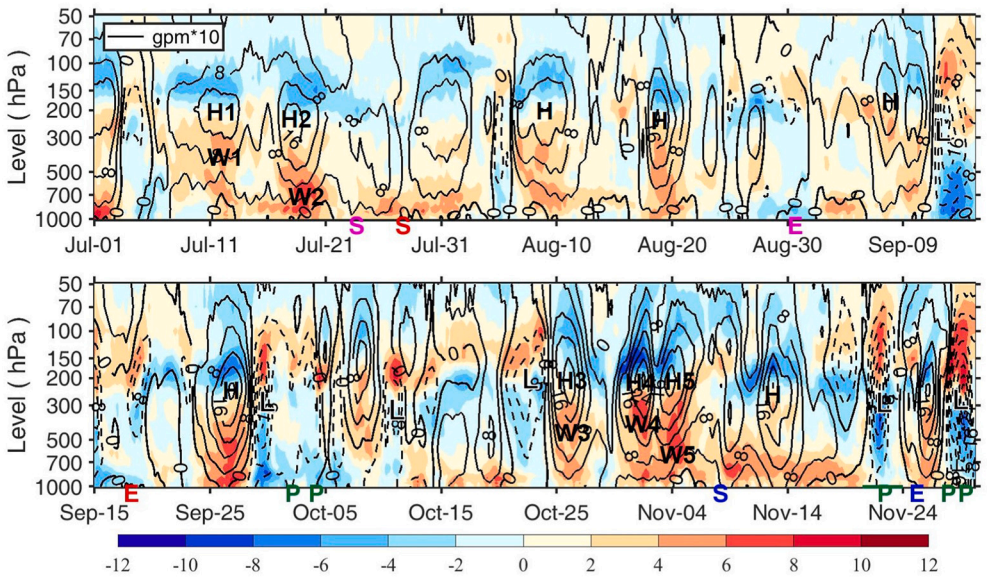

Fig. 4. The hovmoller diagram of GPH anomalies (contour, 4 × 10gpm interval) and temperature anomalies (shading, 2 °C interval) averaged over the box (39–41°N and 122–124°W) from 1 July to 30 November 2018 and between 1000 and 50 hPa. The letters S and E indicate the start and extinguishing dates of the three wildfires respectively (CARR in magenta, MENDOCINO in red, and CAMP in blue), while the green letter P indicates the date of the daily precipitation exceeded 10 mm. The letters H and L indicate high (positive) and low (negative) centers of GHP anomalies, while the letters W and C indicate warm (positive) and cool (negative) centers of temperature anomalies. (For interpretation of the references to color in this figure legend, the reader is referred to the web version of this article.)

Table 1
Central values of positive (>160gpm inclusive) and negative (<−160gpm, inclusive) LGA, in which the negative values are shown in bold-italics.

No.	Date (Month-day-hour)	Intensity (gpm)
1	Jul-18-12	178.4
2	Aug-08-18	160.7
3	Aug-18-18	204.9
4	Sep-07-18	164.9
5	Sep-13-06	***−179.6***
6	Sep-27-06	205.5
7	Sep-30-06	***−207.4***
8	Oct-26-18	221.9
9	Nov-02-00	288.3
10	Nov-04-12	258.6
11	Nov-13-06	242.1
12	Nov-22-12	***−247.6***
13	Nov-26-18	203.9
14	Nov-29-18	***−362.7***

3. Three large wildfires in 2018

The top 20 largest wildfires listed on the CAL FIRE website are numbered from different decades. The decadal numbers of them are 7, 8, 1, 1, 2, and 1 respectively in the 2010s, 2000s, 1990s, 1980s, 1970s, and 1932. Fifteen large fire cases happened in the most recent two decades. During the 1970s, 1980s, and 1990s, only 4 large fire cases occurred while there was no large fire case from the 1940s to 1960s. This increasing trend of large wildfire numbers may be associated with long-term fuel conditions, human activity, and climate warming (Goss et al., 2020; Mass and Ovens, 2019; Swain, 2021; Williams et al., 2019). Among these 20 large cases, 7 were caused by lightning, 6 were linked to human related activity, 2 were associated with power lines, 3 were under investigation and 1 was undetermined.

In 2018, the burned area of wildfires was the largest since 1932, and three of them were listed at the Top 20 table of the California large wildfires. The first one is the CARR Fire, which is the 7th largest fire in

Table 2
Central values of positive (>6 °C) and negative (<−6 °C, included) ATA averaged vertically from 1000 hPa and 500 hPa, in which the negative values are shown in bold-italics.

No.	Date (Month-day-hour)	Intensity (°C)
1	Jul-01-06	10.19
2	Jul-19-06	7.22
3	Jul-26-18	6.32
4	Jul-29-12	6.56
5	Aug-18-12	6.19
6	Sep-13-06	***−8.51***
7	Sep-27-12	9.24
8	Sep-30-12	***−8.32***
9	Oct-13-12	6.75
10	Oct-20-12	7.41
11	Nov-05-00	8.62
12	Nov-09-12	7.29
13	Nov-15-12	6.27
14	Nov-17-00	6.09
15	Nov-22-12	***−7.15***
16	Nov-29-18	***−6.54***

ranking, happened in Shasta County and Trinity County from 23 July to 30 August 2018. The burned area reaches 229,651 acres within 39 days. It took seven lives and destroyed 1604 structures. The second one is the Mendocino Complex Fire, which is the largest case on record, burned in Mendocino, Glenn, Lake, and Colusa Counties. The burned area was 459, 123 acres in 54 days from 27 July to 18 September 2018. One person died in the wildfire and 280 structures were ruined. The third one is the Camp Fire in Butte County, which is ranked 16th by area. In the burned area of 153,336 acres, 86 people and 18,804 structures were engulfed in the fire within 18 days from 8 to 25 November 2018, which is the deadliest and most destructive wildfire in the history of California (Silveira et al., 2021).

In this study, we will analyze these three large wildfires. Fig. 1 shows the affected counties of the three cases, which all occurred near mountain regions. In the summer (June–July-August) of 2018, precipitation in northern California was much less than its climatology (Figs. 1 and 2a), which increases the risk of wildfires. The area burned by the deadliest case during 8–25 November 2018 in Butte County is the smallest among the three cases. Although it had been aggravated and extended rapidly by the downslope flows at first, the fire came under control after the help of heavy rain on 21–24 November 2018 (color bar in Fig. 1).

Two large wildfires, the CARR Fire and the MENDOCINO COMPLEX Fire started from 23 and 27 July 2018 (Fig. 1), when the climate of maximum surface air temperature (Tmax) reaches the seasonal peak 35 °C (red line in Fig. 2a). For the coastal station (No. 49699), its seasonal temperature is peaked at 20 °C in the middle of August. These two fires occurred in the period of seasonal warm-dry climate (high Tmax and low precipitation) from July to August in the inland stations (red line and green bar in Fig. 2a). However, the third wildfire was started from 8 November and persisted to 25 November 2018 when seasonal maximum temperature is lower than 20 °C and daily-mean precipitation is climatologically more than 2 mm/day. Therefore, the seasonal warm-dry climate is not the sole determining factor for every large fire.

Fig. 2b shows the four inland station time series of monthly-mean maximum temperatures in July in northern California from 1989 to 2018. The long-term temperature trend is 0.35 °C/decade for the four inland stations and their interannual variability is similar. But the long-term reducing trend (−0.87 °C/decade) is seen at the coastal station (FT BRAGG 43161). The spatial trends agree that anthropogenic global warming will warm the interior more than the coastal zone (Hughes et al., 2009). Their long-term warming trend averaged from the four inland stations has an increased maximum temperature about 1.044 °C during the last 30 years. The monthly-mean departure of maximum temperature during 2017 and 2018 relative to its climate in July is only about 0.6 °C, which is much smaller than the inter-annual variation from their standard deviation (1.64 °C) and also smaller than the long-term inland warming trend. The other 4 large wildfires started in July are found in 1977, 2002, 2007, and 2015. Only except for 2002, July maximum temperature in 2007 and 2015 was also close to the long-term climatology, similar to in 2017 and 2018 (Fig. 2b). We also examined the long-term trends of monthly-mean maximum temperature in June and August in northern California with the increased value of 3.153 °C and decreased value −0.747 °C respectively for the last 30 years (figures not shown). These showed that the long-term temperature trends are different and even opposite from month to month in northern California. Although the long-term warming trend could be responsible for the increase in area burned (Williams et al., 2019), we need to find other possible critical conditions for the explanation of the three large wildfire spreads in 2018.

The progress of the three large wildfires is shown in Fig. 3. The active fire area is represented by the color bar whereas the burned area is indicated by the grey bar. Running total burned area in the MENDOCINO COMPLEX Fire increased from 5000 to 9000 and 16,500 acres per day in the first 3 days (Fig. 3a). The burned area in the CARR Fire increased from 1500 to 1600 and 3600 acres per day in the first 3 days (Fig. 3b). However, the CAMP Fire burned rapidly in the first 3 days with an increase of area from 20,000 to 70,000 and 15,000 acres per day (Fig. 3c), which is a rare situation. These varying burned speeds and fire propagation may be affected by different fuel and meteorological conditions including strong northerly winds in the mountain regions.

4. General evolutions of vertical anomalous variables

In previous studies, favorable weather conditions for forming California wildfires were considered at a certain level or several levels in the lower troposphere by commonly using conventional or total synoptic analysis methods. For example, Miller and Schlegel (2006) used the surface pressure fields to study the 19–22 December 1999 Santa Ana fires, Abatzoglou et al. (2013) used the mean sea level pressure, mean temperature advection, and mean winds at 850 hPa to study the most notorious fire-weather conditions in southern California, Cao and Fovell (2016) used the 700 hPa winds to study the wildfires at San Diego County, and Peterson et al. (2015) studied the 500 hPa cut-off low system in the 2013 Rim Fire case. Recently, Mass and Ovens (2019) used the low-tropospheric multilevel (surface, 950, 850, 700, and 500 hPa) variables to analyze the northern California wildfire case of 8–9 October 2017. It is understandable that certain synoptic patterns in the lower troposphere should exhibit a suitable condition for fire spread. In this study, we would like to compare the different patterns in the whole atmosphere, indicating California's large wildfires, between using conventional and anomaly-based synoptic analyses. We draw the hovmoller diagram of total GPH and temperature averaged over the burned area of wildfires (i.e., the box: 39–41°N and 122–124°W) in northern California from 1 July to 30 November 2018 (not shown). From the troposphere to the stratosphere between 1000 hPa to 50 hPa, there were many fluctuations of temperature with some large amplitudes between the upper troposphere (150–300 hPa) and the stratosphere (above 150 hPa) but no intuitional signals indicating the three fires can be observed from the total GPH during this five-month period. However, Fig. 4 shows the hovmoller diagram of GPH and temperature anomalies averaged over the same box area from 1 July to 30 November 2018. From the entire atmosphere between 1000 hPa to 50 hPa, it is clear that the largest signals are GPH anomalies located at the upper troposphere. The CARR and MENDOCINO wildfires started on 23 July and 27 July respectively and are indicated by the letter S in Fig. 4. Before the ignitions, two positive centers (H1 and H2) of GPH anomalies occurred in the upper troposphere. Beneath each positive center of GPH anomalies, there was a warm-air column of temperature anomalies extending in the middle troposphere to the surface. The warm-air mass anomalies (W1 and W2), indicated by red shading columns in the mid-to-low troposphere (below 300 hPa), provide favorable conditions for drying air and fire spread

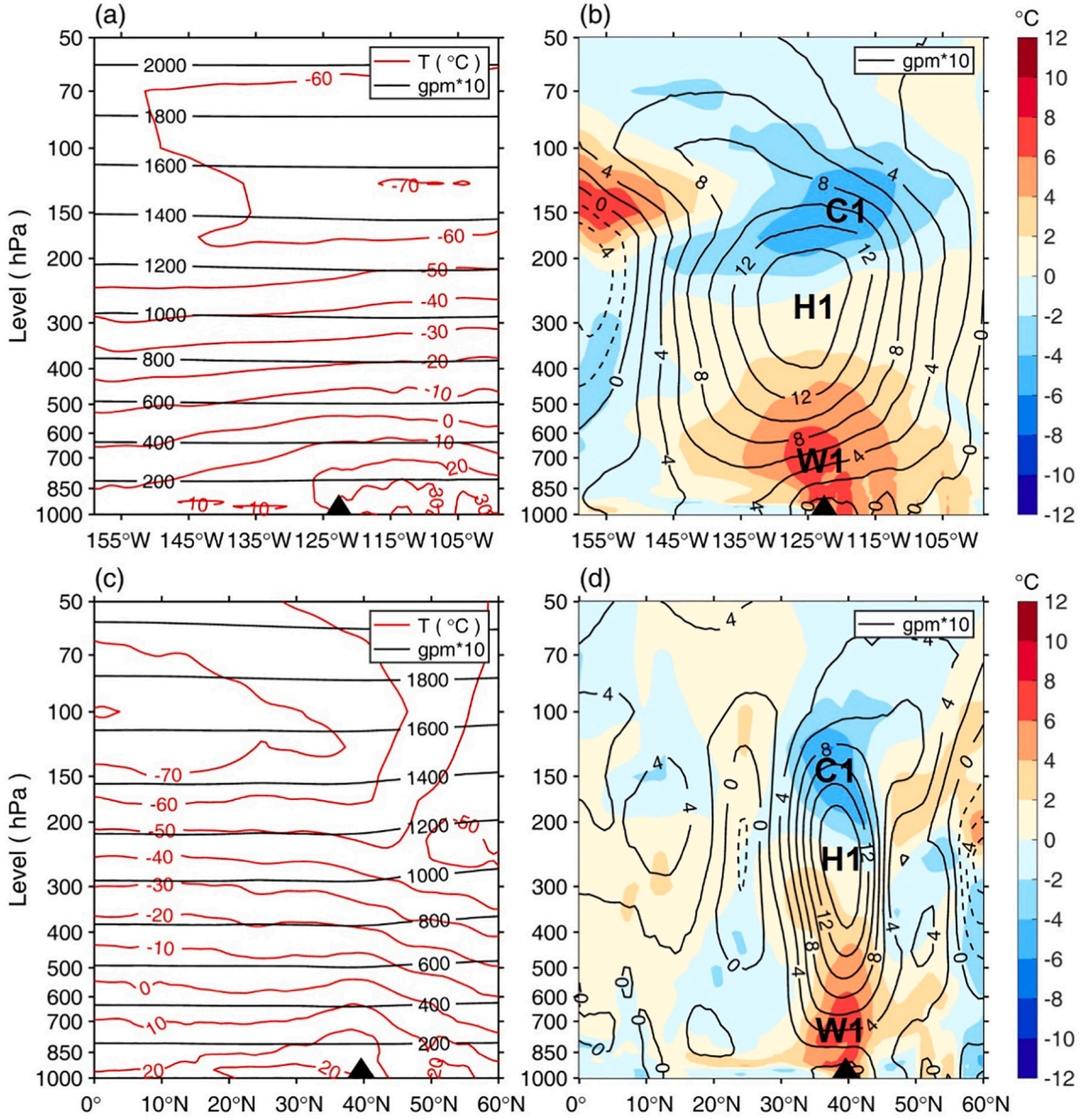

Fig. 5. The vertical cross-sections of (a) total height (black contour, 200 × 10gpm interval) and total temperature (red contour, 10 °C interval), (b) geopotential height anomaly (contour, 2 × 10gpm interval) and temperature anomaly (shading, 2 °C interval) along 39.75°N and between 1000 and 50 hPa at 0600 UTC on 19 July 2018 (4 days prior to the start of CARR fire and 8 days prior to the start of MENDOCINO fire), and (c) and (d) are same as in (a) and (b) only except along 123°W. The letters H and L indicate the high (positive) and low (negative) centers of GPH anomalies or the LGA centers while the letters W and C indicate warm (positive) and cool (negative) centers of temperature anomalies or the ATA centers. The black triangles indicate the longitude (latitude) of the general area of both CARR and MENDOCINO wildfires. (For interpretation of the references to color in this figure legend, the reader is referred to the web version of this article.)

prior to the fire events. Due to the hydrostatic balance, the GPH and temperature anomalies always appear in a pair and form a deep vertically coupled anomalously temperature pattern to indicate potential fire spread. The two warm-air mass centers of temperature anomalies in middle July became even clearer in the normalized anomalies (figure not shown).

Before the CAMP Fire on 8 November 2018, three positive centers of GPH anomalies (H3 on 26 October, H4 on 2 November, and H5 on 4 November) occurred at the upper troposphere together with three warm-air mass centers (W3, W4 and W5) of temperature anomalies at the mid-to-low troposphere (Fig. 4). These anomalous warm-air masses added a seasonal warm-dry cycle in the mid-to-low troposphere could consecutively accumulate the dry static energy and dried vegetation, which are stronger than the long-term warming trend for the fires. The centers of anomalous warm-air mass higher than 6–10 °C are the critical signal from the anomalous synoptic component which is suitable for fire spread. After the CAMP Fire event started, two additional anomalous warm-air mass centers followed. These anomalous weather conditions, combined with a heavy fuel loading, can explain why the wildfire rapidly spread particularly during the first 2 days. This wildfire extinguished on 25 November 2018 when an anomalous cold-air mass center with rain passed from 21 to 24 November 2018, as indicated by the letter P in Fig. 4 and the color bar in Fig. 1. The analysis of normalized anomalies (relative to climatological standard deviation SD) is even clearer to indicate the intensities of warm-air and cold-air masses (not shown). Several anomalous warm-air masses (with exceedance of 2 SD) appeared before the starts of the large wildfires, while the negative center of GPH anomaly (with their values less than −1.2 to −1.6 SD) and the negative center of temperature anomaly (with their values lower than −2 SD) occurred before their extinguishing.

Jiang et al. (2016) did a comparison study between the two forms of anomalies, i.e., relative and normalized anomalies. They both have pros

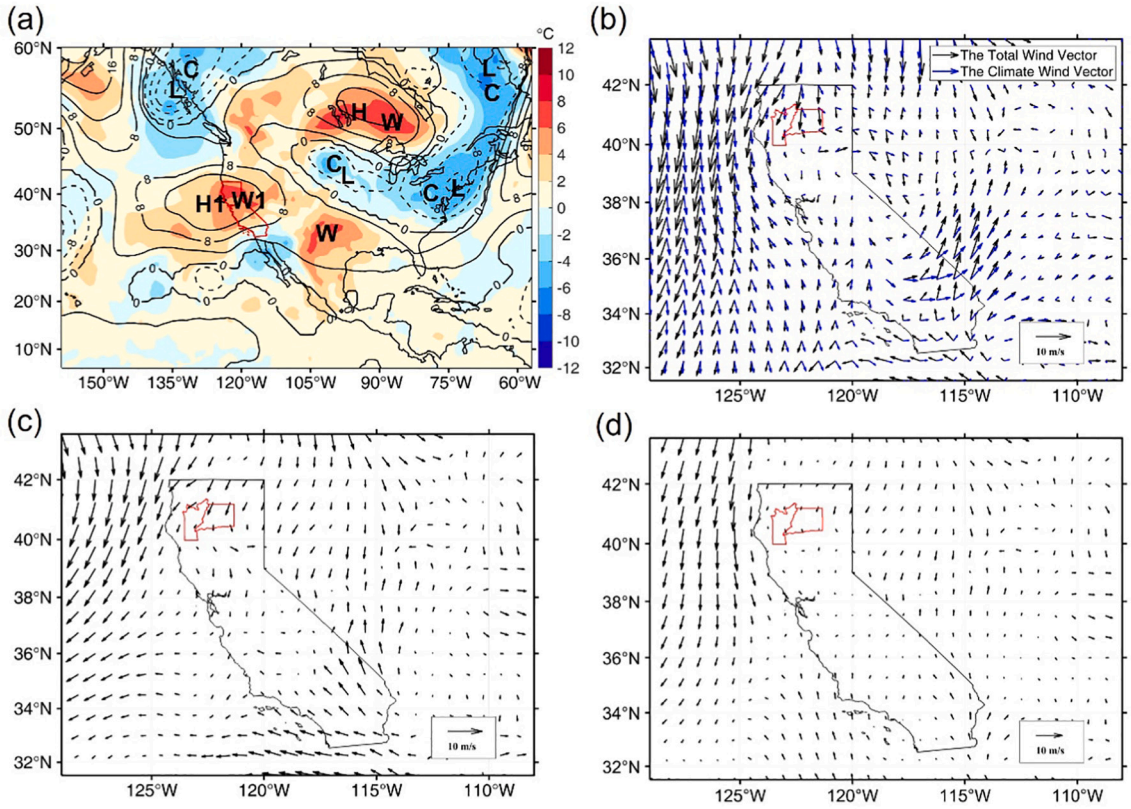

Fig. 6. (a) The horizontal distributions of LGA (contour, 4 × 10gpm interval) extracted from 500 to 200 hPa and temperature anomalies (shading, 2 °C interval) at 850 hPa at 0600 UTC on 19 July 2018 (4 days prior to the start of CARR fire and 8 days prior to the start of MENDOCINO fire). The letters H and L indicate the high (positive) and low (negative) maximum LGA centers of GPH anomalies while the letters W and C indicate warm (positive) and cool (negative) centers of temperature anomalies at 850 hPa. The red line in (a) covers the state of California. (b) The horizontal distributions (10 m/s) of total wind (black vector) and climatic wind (blue vector) at 850 hPa at 0600 UTC on 19 July 2018. (c) Same as in (b) except for anomalous wind. (d) Same as (c) but at 1000 hPa level. The red area in (b), (c) and (d) are the counties affected by the wildfire. (For interpretation of the references to color in this figure legend, the reader is referred to the web version of this article.)

and cons. Since hydrostatic relation is valid in relative anomaly but not in normalized anomaly, the relative anomaly will be used in the rest of this study. In Fig. 4, the largest geopotential anomaly (LGA) with only a positive or negative value at the box or any grid can be vertically obtained from the entire atmosphere between 1000 and 50 hPa. Table 1 lists the positive and negative LGA centers with their central values larger than 160 gpm or less than −160 gpm. Among the 14 LGA centers identified from July to November of 2018, only 4 of them are negative centers and others are positive centers. It indicates that positive LGA centers occurred more frequently than negative ones in the region of northern California during this period. All these centers of GPH anomalies were located at the upper troposphere rather than at 500 hPa or in the lower troposphere which was commonly selected by many previous studies (Abatzoglou et al., 2013; Cao and Fovell, 2016; Peterson et al., 2015).

Fig. 4 also shows that beneath each of the positive LGA centers there exists a warm-air mass of positive air temperature anomaly (ATA) at the mid-to-low troposphere. These ATA centers are warm-air mass anomalies in the mid-to-low troposphere which hit the surface and increase the risk of fire. Table 2 lists the positive central value (>6 °C) and negative central value (<−6 °C) of ATA averaged vertically from 1000 hPa and 500 hPa. Among the 16 ATA centers identified, 12 of them are anomalous warm-air mass centers but only 4 are anomalous cold-air mass centers. The higher frequency of anomalous warm-air mass centers in the mid-to-low troposphere provides an anomalous weather condition favorable for wildfire spread. Before the two fire ignitions on 23 (CARR) and 27 (MENDOCINO) July 2018 (marked by a magenta and a red letter S, respectively), there were two anomalous warm-air mass centers (W1 and W2) on 11 July and 19 July 2018. The three anomalous warm-air mass centers on 29 July, 9 August and 18 August 2018 should be anomalous weather conditions further enhancing these two wildfire spreads. The extinguishing of the CARR fire on August 30 was apparently associated with the weak but lasting (25 August – 1 September) negative temperature anomaly. The cold-air mass center of negative temperature anomaly centered on 13 September 2018 is a weather condition for the extinguishing (marked by a red letter E) of the MENDOCINO wildfire on 18 September 2018. The third large CAMP wildfire, which started on 8 and persisted to 25 November 2018 (from the blue letters S to E), was preceded by three anomalous warm-air mass centers (i.e., W3, W4, and W5 in Fig. 4) before its ignition and was accompanied by other three positive ATA centers during the burned period (Table 2). An anomalous cold-air mass center with rain centered on 22 November 2018 was a weather condition for the CAMP fire extinguishing. Fig. 4 reveals that mid-to-low troposphere anomalous warm-air and cold-air mass centers induced by upper-troposphere GPH anomalies are critical atmospheric patterns potentially affecting the fire spread and extinguishing in northern California.

5. Anomalous synoptic patterns for the first two wildfires (CARR and MENDOCINO)

Anomalous warm-air masses are “warm anomalies” in the mid-to-low troposphere as an indicating factor favoring wildfire spread in a future time as shown in Fig. 4. The aloft warm-air mass anomaly can cause surface pressure anomaly and surface wind anomaly (downslope wind), which is commonly observed for severe wildfires (Mass and Ovens, 2019). In Table 2, we list the date and time when large positive or negative ATA central values occurred during July through November of

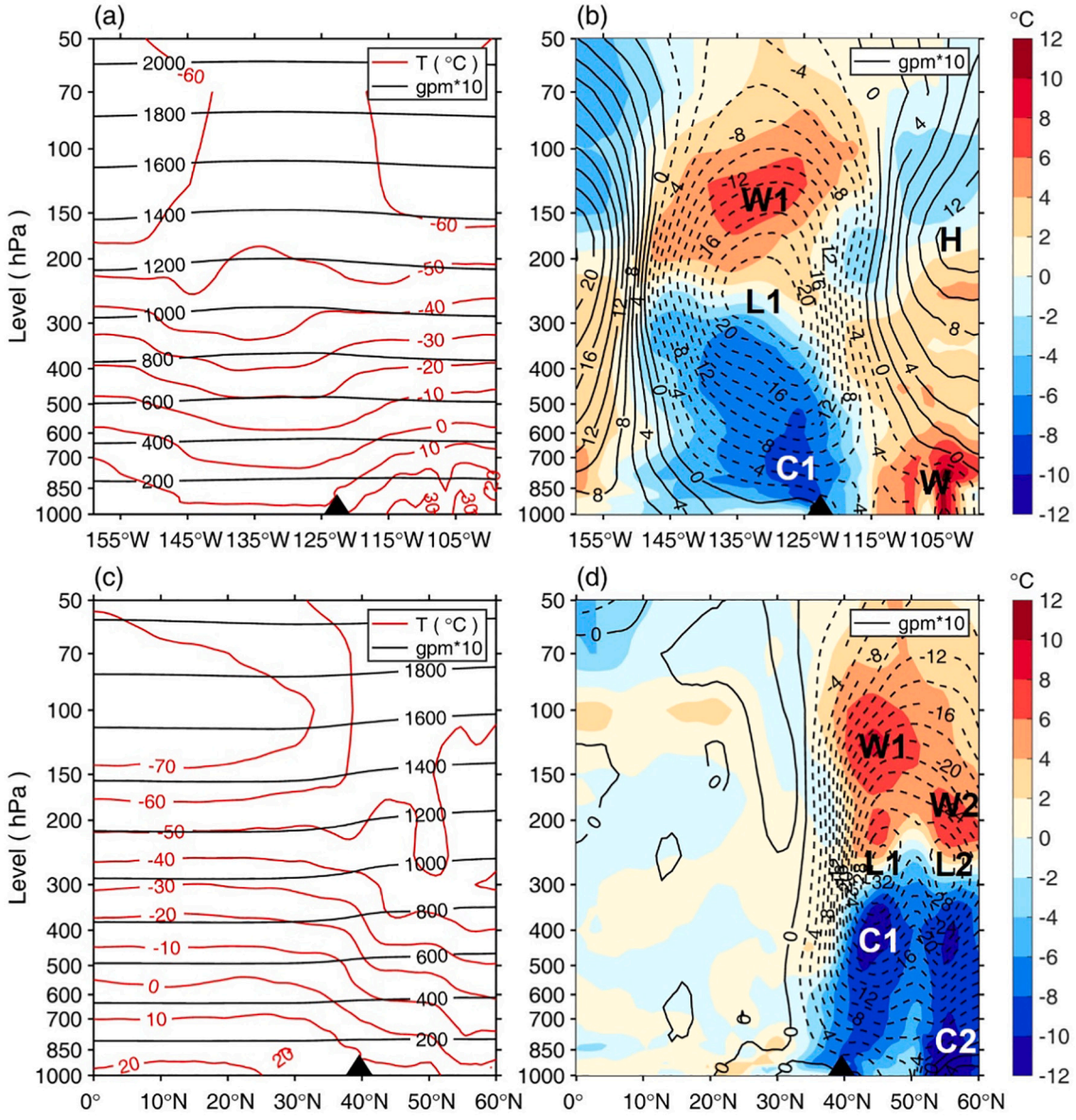

Fig. 7. Same as in Fig. 5 except at 0600 UTC on 13 September 2018 (5 days prior to the extinguishing of MENDOCINO fire).

2018. Before the first two wildfires started on 23 (CARR) and 27 (MENDOCINO) July 2018, there was a moment at 0600 UTC on 19 July 2018 when the intensity of positive warm-air anomaly reached 7.22 °C. At that precursor moment, we compare in Fig. 5 with the total and anomalous variables in the vertical cross-section along 39.75°N and 123°W. The total height and total temperature shown in Fig. 5a and c do not give an obvious pattern potentially for coming wildfire spread. In contrast, Fig. 5b and d clearly reveal positive and negative centers of GPH anomalies as well as vertically coupled warm-air and cold-air mass centers of temperature anomalies. These anomalous centers are collocated with the location where the two fires occurred 4 and 8 days later. The warm-air mass anomaly in the mid-to-low troposphere with a surface shallow low and the positive center of GPH anomalies or the positive LGA center (H1) at the upper troposphere constructs a vertical pattern for potential large wildfire in northern California. The surface shallow low over inland and high pressure near the coast form an anomalous horizontal pressure gradient which results in anomalous northerly wind (Fig. 5b). This anomalous synoptic pattern is a specific condition for the ground anomalous downslope wind (Fig. 6c and d) that actually drives wildfire and that fire fighters need to respond to.

Fig. 6a shows the horizontal distributions of LGA extracted from 500 to 200 hPa and the temperature anomalies at 850 hPa on 0600 UTC on 19 July 2018. There were many LGA centers as well as warm-air and cold-air mass centers of temperature anomalies at 850 hPa, which move eastward slowly (not shown). Over the wildfire areas, there was a positive LGA center (H1) and an anomalous warm-air mass center (W1) at 850 hPa. This anomalous synoptic pattern, superposed to the long-term warming trend and seasonal warm-dry cycle, greatly enhanced the anomalous weather condition that drove the fire spread.

Strong downslope winds can foster a rapid spread of wildfires with hot and dry weather conditions leading up to large-scale fire events (Westerling et al., 2004). In mountain regions, downslope flows during dry and hot periods can either directly cause or rapidly spread wildfires (Cao and Fovell, 2016; Mass and Ovens, 2019; Nauslar et al., 2018). The anomalous flow influenced the wildfire area was indeed northeasterly winds at 850 hPa and 1000 hPa, blowing from the continent to the Pacific (Fig. 6c and d). This anomalous offshore flow from the inland mountain region to the Pacific is usually accelerated due to the downslope terrain and becomes hot and dry, all of which contribute to the spread of wildfire. At 0600 UTC on 19 July the climatic flow is very weak

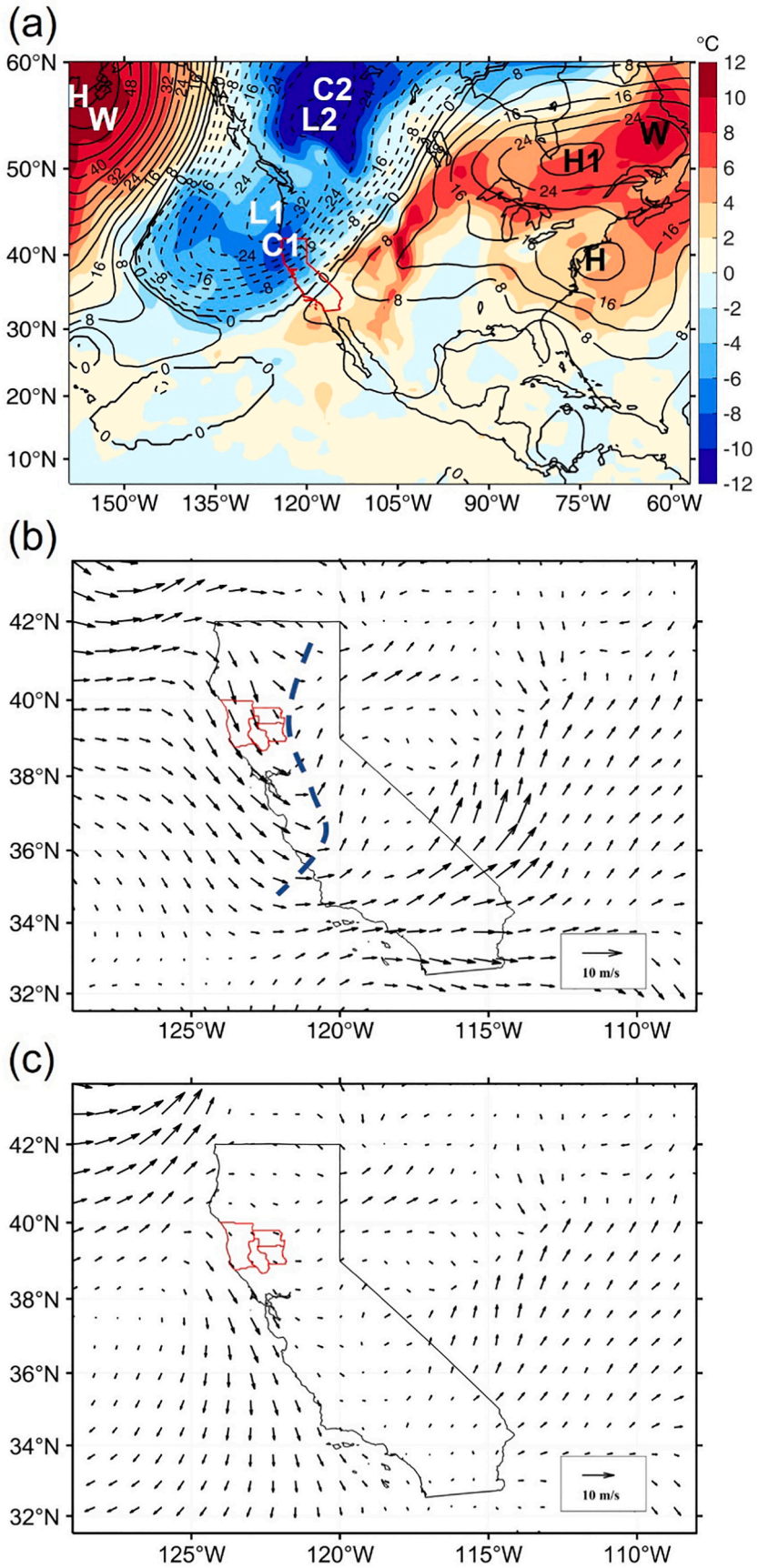

Fig. 8. (a) Same as in Fig. 6a, (b) same as in Fig. 6c, and (c) same as in Fig. 6d except at 0600 UTC on 13 September 2018 (5 days prior to the extinguishing of MENDOCINO fire). In (b) the dashed line is the shear of anomalous flow at 850 hPa.

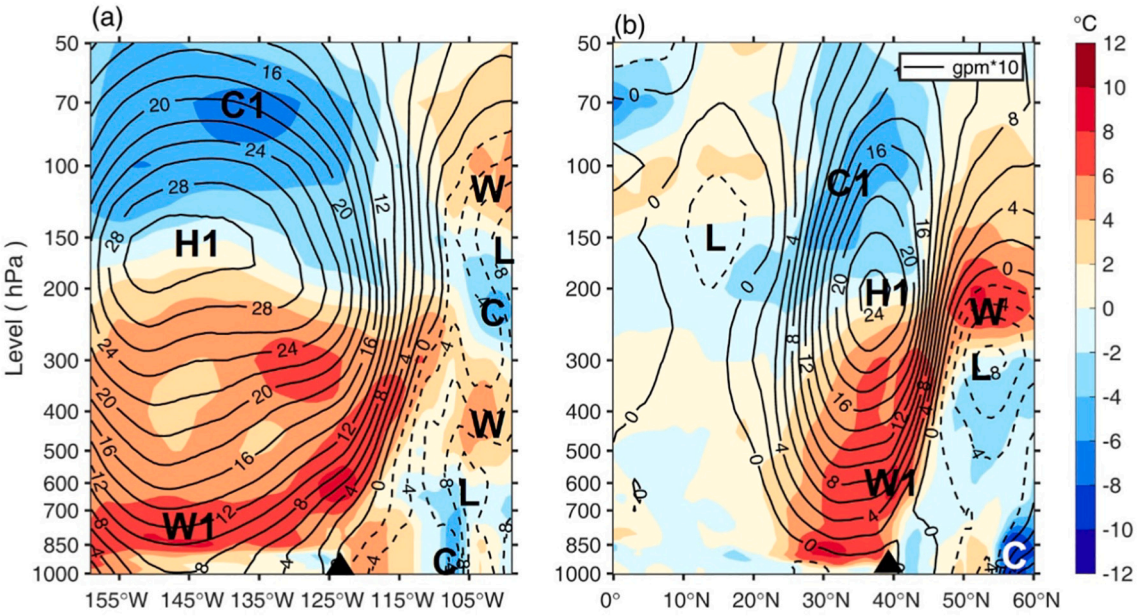

Fig. 9. Same as in Fig. 5b and d except at 0000 UTC on 5 November 2018 (3 days prior to the start of CAMP fire). The black triangles indicate the longitude (latitude) of the general area of the CAMP fire.

showing a northerly wind and, therefore, the total northeasterly wind indicated by the black vector in Fig. 6b is mainly contributed by an anomalous one in Fig. 6c. Wildfire spread is an extreme happened under favorable anomalous weather conditions including the anomalous warm-air mass and the downslope flow in the lower troposphere.

Table 2 also shows an anomalous cold-air mass with a central value of −8.51 °C (exceeding 2 SD of climate variation) at 0600 UTC on 13 September 2018, which is 5 days before the second fire (MENDOCINO) extinguished on 18 September 2018. We compare in Fig. 7 the total and anomalous variables in the vertical cross-sections along 39.75°N and 123°W at 0600 UTC on 13 September 2018. Again, the total GPH and temperature (Fig. 7a and c) do not give clear signals of the fire extinguishing. In contrast, the GPH and temperature anomalies (Fig. 7b and d) reveal an opposite pattern against the fire spread (Fig. 5). Along the zonal direction, a negative LGA center occurred in the upper troposphere right over the fire. An anomalous cold-air mass and an anomalous warm-air mass can be found below and above the negative LGA center, respectively. The anomalous cold-air mass in the mid-to-low troposphere is a potential weather condition for extinguishing the fire. Along the meridional direction, there were two negative LGA centers located in the upper troposphere from 40°N to 60°N. Above and below the two negative LGA centers were two anomalous warm-air masses in the stratosphere and two anomalous cold-air masses in the mid-to-low troposphere. This 3-dimensional GPH-temperature anomalous pattern is vertically coupled to each other in the whole atmosphere and cannot be separated from the stratosphere to the troposphere.

Fig. 8 depicts the horizontal distributions of LGA extracted from 500 hPa to 200 hPa superimposed on the temperature anomalies at 850 hPa at 0600 UTC on 13 September 2018 (5 days prior to the extinguishing of the MENDOCINO fire). The two anomalous cold-air masses in Fig. 7d (i.e., C1 and C2) can be clearly seen in Fig. 8a. The wildfire area was particularly influenced by the negative LGA center L1 and the cold-air mass anomaly C1 in northern California. Another negative LGA center L2 with cold-air mass anomaly C2 was located in mid-west Canada. These anomalous synoptic systems move eastward slowly (not shown). In the meantime, anomalous onshore flows at 850 hPa and 1000 hPa blow from the northeast Pacific toward California (Fig. 8b and c). The anomalous onshore flows bring a cold-wet air mass to the continent with a shear extending southward along the central part of northern California. This deep low system of GPH anomalies with anomalous cold-air mass in the mid-to-low troposphere provides an anomalous weather condition inhibiting wildfires, which leads to the MENDOCINO fire extinguishing in northern California. Spatial distribution of all anomalous variables from Figs. 5–8 indicated that an important signal directly linked to fire weather conditions is situated in the whole atmosphere from the troposphere to the stratosphere. Thus, a wildfire is associated with a spatial pattern of temperature-height anomalies.

6. Anomalous synoptic patterns for the third wildfire (CAMP)

The third large wildfire (CAMP fire) occurred in a non-wildfire season (8–25 November 2018) and behaved differently from the previous two cases given its rapid spread during the first 2 days. In spite of its uniqueness, the large-scale anomalous pressure-temperature pattern that we saw in the previous two wildfires still fits the third case. As mentioned in Fig. 4, there were three positive LGA centers and three anomalous warm-air masses passed over the wildfire area from 26 October to 4 November 2018. The nearest LGA center occurred over northern California on 4 November 2018, which was 4 days before the fire started. The LGA-induced anomalous warm-air mass can be seen as a potential anomalous weather condition to the rapid spread of wildfire through the ground wind (Fig. 10b and c). The positive ATA peaked at 0000 UTC on 5 November 2018 (+8.65 °C, Table 2) prior to the deadliest fire ignition only for 3 days.

Fig. 9 shows the anomalous variables in the vertical cross-sections along 39.75°N and 123°W at 0000 UTC on 5 November 2018 (3 days before the CAMP fire starts). It reveals that an anomalous warm-air mass was located northwest of the wildfire area beneath a very strong positive LGA center. A deep system of positive GPH anomalies extended from the surface to the upper stratosphere with the positive LGA center at 150 hPa is located to the west of the CAMP fire area. The anomalous warm-air mass extending deeply from the surface to 200 hPa implies that there was a potential anomalous weather condition for wildfire over the area. This large anomalous warm-air mass in the troposphere sits beneath a large anomalous cold-air mass in the stratosphere. This anomalous unstable thermal structure could enhance anomalous energy release and cause strong northerly winds (dry-hot foehns) in northern California, which favors a rapid fire spread.

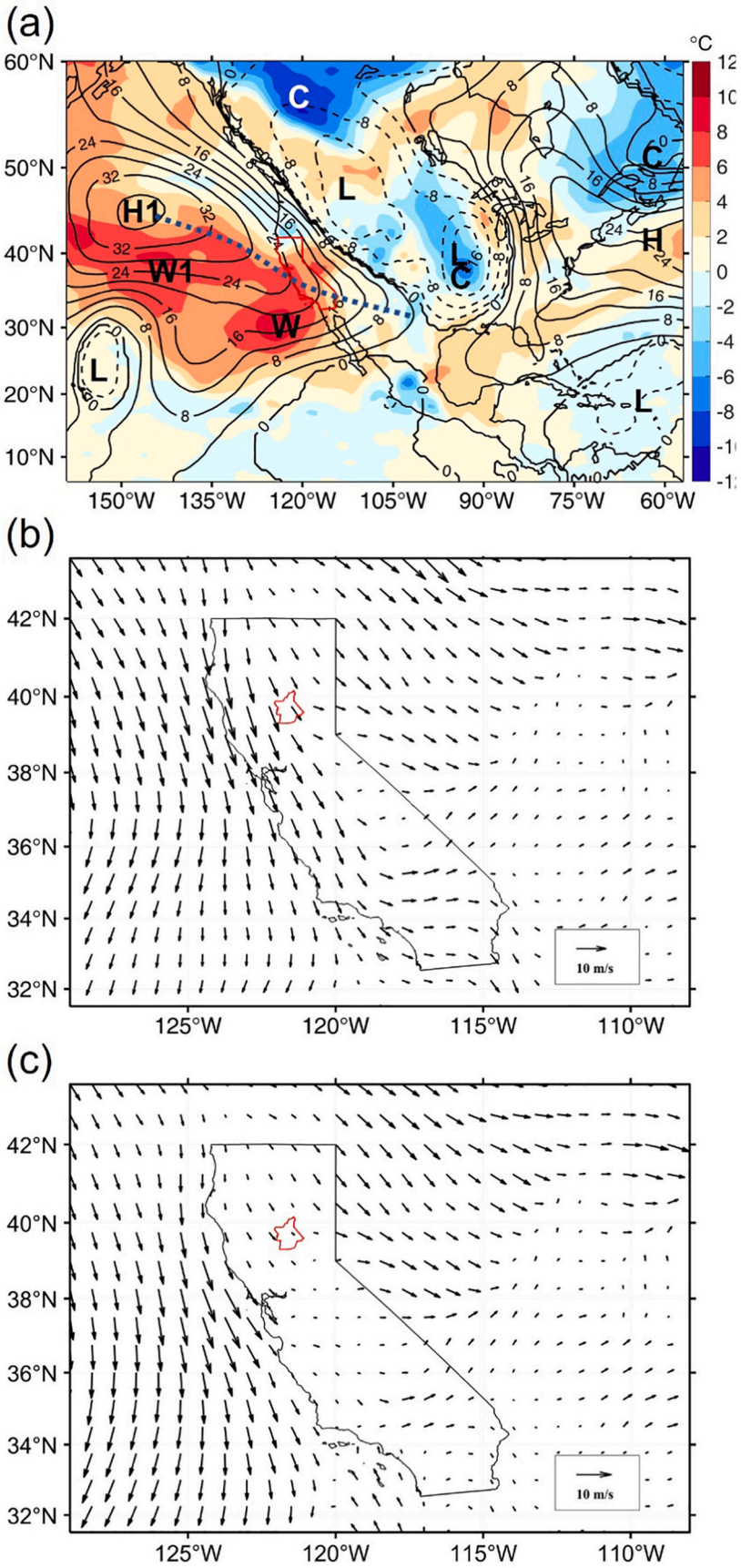

Fig. 10. Same as in Fig. 8 except at 0000 UTC on 5 November 2018 (3 days prior to the start of CAMP fire). The heavy dotted line is the ridge of positive LGA in (a).

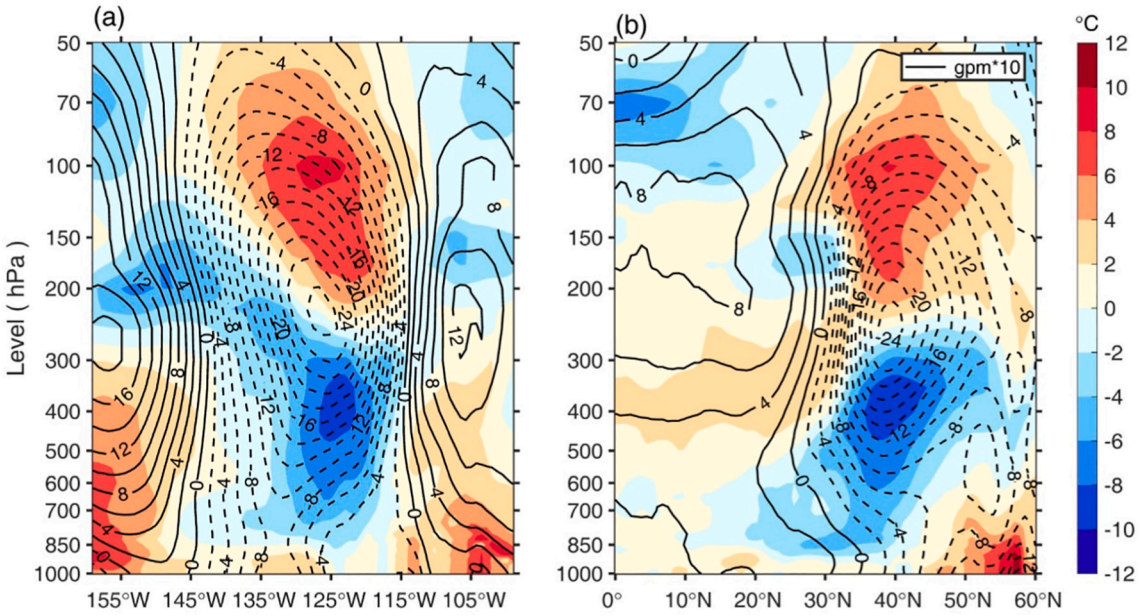

Fig. 11. Same as in Fig. 5b and d except at 1200 UTC on 22 November 2018 (3 days prior to the extinguishing of CAMP fire).

The relative location of LGA centers and anomalous warm-air mass can be seen in Fig. 10a. The positive LGA center H1 and the anomalous warm-air mass center W1 were collocated in the northeast Pacific near the west coast of the North American continent. The wildfire area was potentially influenced by the ridge of the positive LGA and the warm-air mass anomaly at 850 hPa. This LGA center moved eastward slowly (not shown). Under this deep system of anomalous anticyclone, the anomalous offshore northerly flows at 850 hPa and 1000 hPa prevailed over the entire California (Fig. 10b and c). This anomalous offshore flow associated with a stronger gradient of horizontal GPH anomalies had a deep structure in the troposphere over the fire area (see Fig. 9a). Over the wildfire area, northerly wind anomalies can persist when the LGA center moved eastward slowly from west to east crossing California. The situation became worse in the coming days due to anomalous warm-air mass and high offshore flow (dry-hot foehns), which explains why the fire area increased rapidly soon after the fire broke.

Most short and weak wildfire events that lasted for only several days can be extinguished by suppression or human forces under weak weather conditions. But large wildfires which occur with favorable weather conditions as those shown in Figs. 6 and 10 can persist for more than 10 days. These large wildfires cannot be extinguished timely by human forces. Its extinguishing must wait until unfavorable weather conditions such as those identified as in Fig. 8 appear. Therefore, anomalous cold-air mass with rainy weather acts as a damping factor for wildfire control although it is not the only reason since fuels and topography also play important roles.

What were the unfavorable weather conditions that had happened before the large CAMP wildfire extinguished? As listed in Table 2, an anomalous cold-air mass with its central value of −7.15 °C occurred at 1200 UTC on 22 November 2018 (3 days prior to the extinguishing of the CAMP fire). Fig. 11 displays the vertical cross-sections of anomalous variables at this moment. A negative center of GPH anomalies centered around 200–250 hPa was located over the wildfire area with an anomalous cold-air mass below and an anomalous warm-air mass above. For this case, the coolest center was situated at 400 hPa rather than at 850 hPa but the negative temperature anomalies persisted in the coming days and extended their influence to the surface. Fig. 12a shows the horizontal distributions of LGA and temperature anomalies at 850 hPa at 1200 UTC on 22 November 2018. A wave-train pattern is clearly observed in the middle latitudes along the 50°N. The region of northern California was influenced by the negative LGA center with an anomalous cold-air mass at the northeast Pacific. This wave-train pattern horizontally shows that the west coast and east coast of the North American continent were cooler than normal while the central continent was largely warmer than normal.

Since large-scale atmospheric flow can be approximated as adhering to hydrostatic and geostrophic balances, the GPH anomalies centered at the upper troposphere will be accompanied by temperature and wind anomalies in the lower troposphere. In Fig. 11, the maximum anomalous wind should locate at the region of large gradient place of GPH anomalies in the mid-to-high troposphere. This anomalous wind can extend to the lower troposphere. Fig. 12a shows the distribution of LGA and the 850 hPa temperature anomalies while Fig. 12b and c are the horizontal distribution of wind anomalies at 850 hPa and 1000 hPa at 1200 UTC on 22 November 2018. The onshore wind anomalies are observed over California with flows coming from the Pacific. The cold and wet flows bring more precipitation to the wildfire region during 21–24 November 2018 (color bar in Fig. 1). The daily precipitation is 21 mm at Oroville (station No. 46521), which is a station nearby the CAMP wildfire. Under this anomalous cold and wet condition, the deadliest and most destructive CAMP wildfire finally distinguished on 25 November 2018.

The CAMP fire case from Figs. 9–12 re-confirmed the general spatial patterns of fire spread and extinguishing which are derived from Figs. 5–8. Therefore, the vertical pattern of GPH and temperature anomalies can be used as a necessary weather condition for potential fire spread and extinguishing in northern California. Currently, some studies focus on the forecasting and simulation of wildfires (Coen et al., 2020; Giannaros et al., 2020; Worsnop et al., 2020). If we apply this method to a model forecast product, we might obtain a clearer early warning signal for a possible wildfire when the model is capable of predicting the anomalous synoptic pattern. Does a current operational NWP model have such ability? We use the ECMWF ensemble model data to demonstrate this for the CAMP fire. Fig. 13 shows the vertical distribution of GPH and temperature anomalies predicted by the ensemble mean forecast of the ECMWF EPS. Fig. 13a is the 7.5-day prediction initiated at 1200 UTC on 28 October and projected to 0000 UTC on 5 November 2018 (3 days prior to the start of the CAMP fire). This predicted anomalous synoptic pattern is fairly well compared with the observed anomaly as shown in Fig. 9b. Fig. 13b is the 7-day prediction initiated at 1200 UTC on 15 November and projected to 1200 UTC on 22

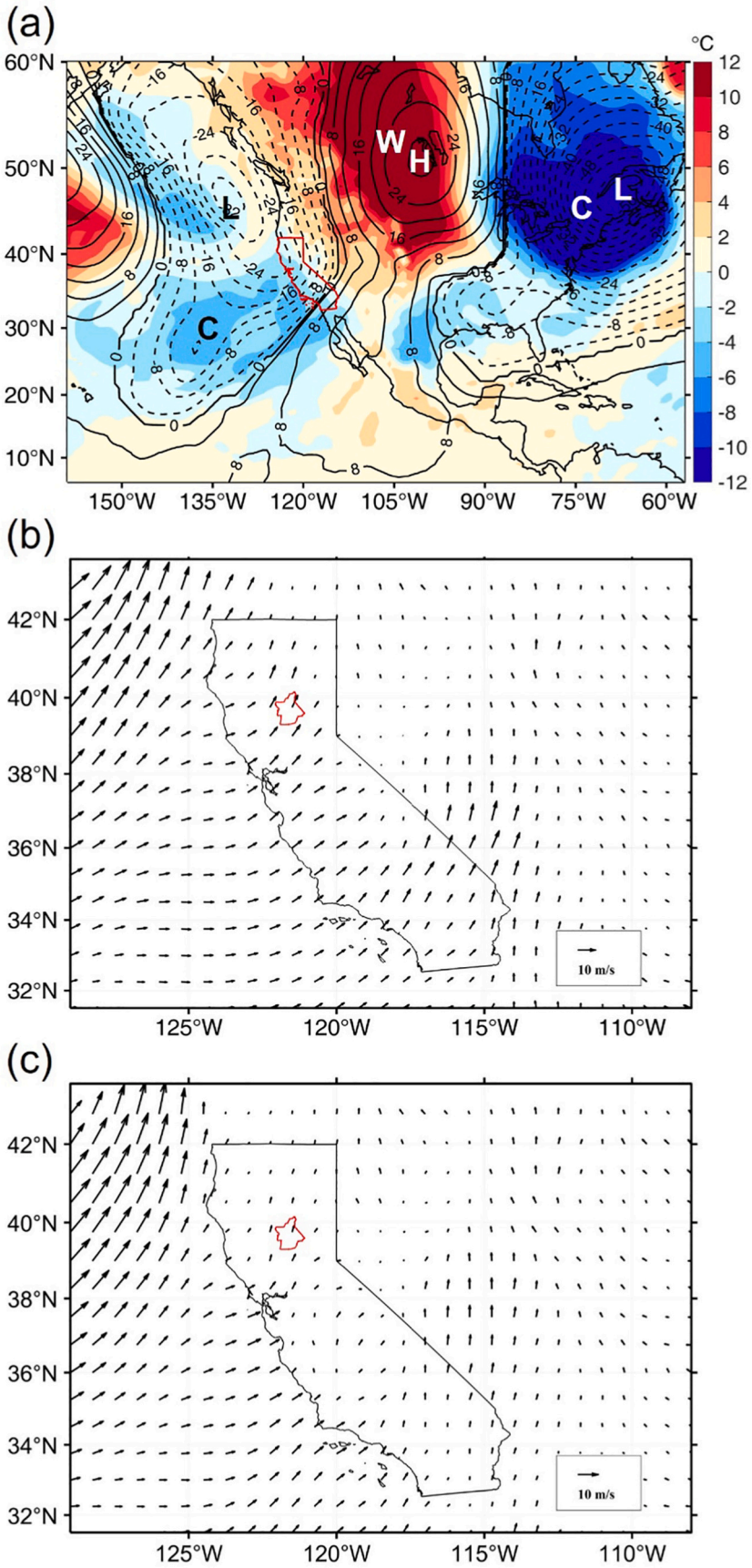

Fig. 12. Same as in Fig. 8 except at 1200 UTC on 22 November 2018 (3 days prior to the extinguishing of CAMP fire).

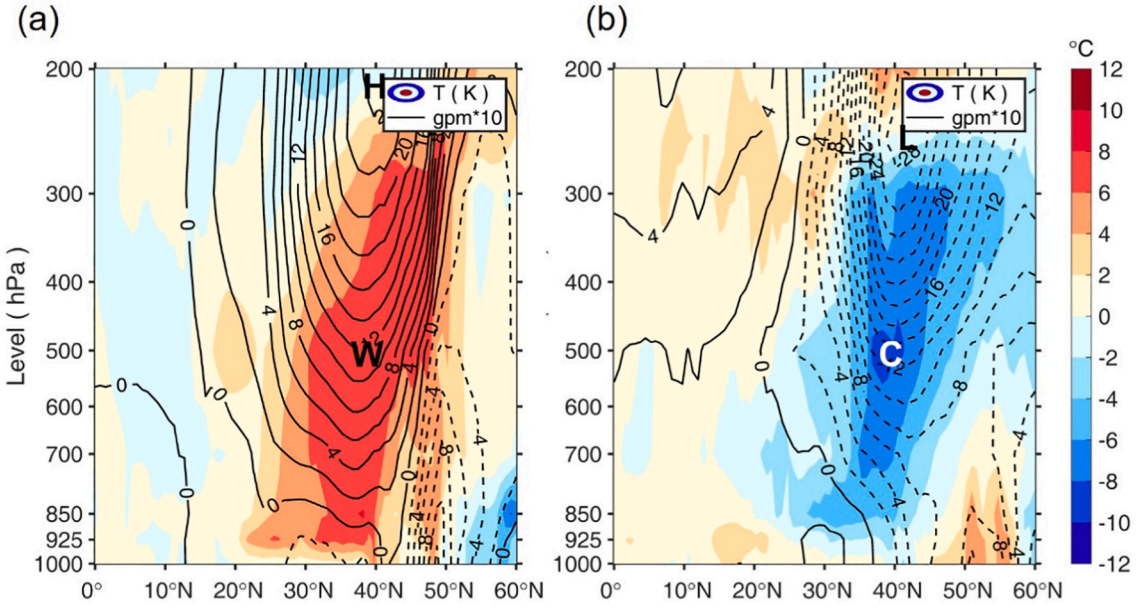

Fig. 13. Same as in Figs. 9b and 11b except of the EPS ensemble mean forecasts: (a) 7.5-day forecast, initiated at 1200 UTC on 28 October and projected to 0000 UTC on 5 November 2018 (3 days prior to the start of CAMP fire); and (b) 7-day forecast, initiated at 1200 UTC on 15 November and projected to 1200 UTC on 22 November 2018 (3 days prior to the extingusing of CAMP fire). (Note that the ECMWF EPS data was provided only to 200 hPa at the highest level so that 200–50 hPa portion cannot be displayed).

November 2018 (3 days prior to the extinguishing of the CAMP fire). Again, this predicted anomalous synoptic pattern is fairly well compared with the observed anomaly as shown in Fig. 11b. This result shows that two opposite synoptic patterns from the analysis of GHP and temperature anomalies for forming and distinguishing the CAMP fire are well predicted by the model with lead times of about 7 days. Therefore, current state-of-the-art operational NWP models could be used in fire-weather prediction by using the anomaly-based approach.

7. Summary and discussions

Wildfire spread needs several conditions. The first condition is fire fuel which is accumulated with time by drought that killed many trees. The second is the thermal condition from the long-term warming trend, summer-autumn warm-dry climate, and individual extreme synoptic anomalies. The third is strong winds near the surface, which can be seen as the dynamical condition. The last two are meteorological conditions. However, the fact shows that large wildfires can ignite and spread in any season, relying on antecedent extreme weather conditions associated with anomalous synoptic patterns. Thus, the answer to our first question is that short-term individual temperature anomalies and wind anomalies near the surface, associated with extreme LGA/ATA centers, are most critical factors for a fire spread and extinguishing and are more important than long-term climate warming trend and seasonal temperature cycle. Major precipitation events play a critical role too in extinguishing wildfire as we showed in this study. Although moisture content in the atmosphere could play a role, we suspect that it will not be a major factor for the following two reasons. One is that California is climatologically a desert-like dry state most of the time (especially from spring to autumn) and its moisture condition in the atmosphere is generally dry enough for wildfires to occur. Another is that atmospheric moisture is a passive variable, which is largely driven by individual weather systems. In other words, its effect should be indirectly accounted for when we describe a pressure-temperature pattern. Therefore, as a first-order factor study for large-scale wildfires, moisture is not included in this study. It will be helpful to be investigated in future studies for small-scale and out-of-season wildfires.

We have identified a 3-dimensional anomalous synoptic pattern of GPH, temperature, and wind which was associated with three major wildfires in 2018 for both fire initiation and extinguishing. A similar result was also found from the analysis of the Thomas Fire occurred in the winter crossing from late 2017 to early 2018 (not reported in this study). These large wildfires occurred in conjunction with a nearby high geopotential height anomaly centered in the upper troposphere, with anomalous warmth in the atmospheric column below this geopotential height maximum. Offshore winds were also seen to occur in association with these fires, associated with higher pressures inland and lower pressures located to the southwest. Two important factors, the anomalous downslope wind and anomalous warm-air column over the ground, are directly linked to the spatial pattern of GPH and temperature anomalies in the atmosphere aloft.

For wildfire extinguishing, the anomalous synoptic pattern is just the opposite against to that of the fire initiation, i.e., anomalous cold-air mass and anomalous onshore winds flowing from ocean to continent in the mid-to-low troposphere. The cold-air mass anomaly in the mid-to-low troposphere is directly associated with a negative center of GPH anomalies or a negative LGA center at the upper troposphere, which appears in the northeast Pacific near the west coast of North America. Under this anomalous cold-low system, onshore winds bring anomalous cold-wet flows from the Pacific to the North American continent to combat the land wildfires.

Frequent synoptic anomalies move eastward along the middle latitude slowly like a wave train and affect northern California from time to time. For those strong anomalous systems, we determined their intensity thresholds of the LGA central value ±160 gpm and the anomalous ATA central value ±6 °C departed from their daily climatology. During 5 months from July to November 2018, a ratio of positive to negative maximum LGA centers is 10:4 and a ratio of positive to negative maximum ATA centers is 12:4. Therefore, consecutive and positive LGA/ATA centers are meteorological conditions before the fire spread. On the other hand, if a large fire has been spreading it will be possibly extinguished soon after a negative LGA/ATA center with a major precipitation event. Thus, how long a large fire could last, as raised in our second question, depends on the time period from fire ignition to negative LGA/ATA occurrence.

The CAMP fire case showed that the anomalous synoptic patterns

have been well predicted before the fire spread and fire extinguishing by the ECMWF ensemble mean forecast at least a week in advance. As shown by Mass and Ovens (2019), they also give the excellent operational forecasts issued for one of the cases in 2017 by leading 36 h. Both works suggest that current operational NWP models could be used for fire weather prediction. Based on this study, if model output products are decomposed into temporal anomalies, strong signals of anomalous synoptic patterns could be revealed. When central LGA/ATA values in an anomalous pattern reach their thresholds, they can be used as an indicator to predict potential large wildfires. A large number of fire cases will be needed to establish a well-constructed and robust threshold-based precondition or fire-weather index for forecasting wildfire to keep both higher accuracy and lower false-alarm rate.

CRediT authorship contribution statement

Weihong Qian: Conceptualization, Methodology, Supervision, Funding acquisition, Writing - Original Draft, Writing – Review & Editing. **Yang Ai:** Visualization, Formal analysis, Resources, Writing – original draft, Validation. **Jin-Yi Yu:** Formal analysis, Investigation, Writing – Review & Editing. **Jun Du**: Formal analysis, Investigation, Writing – Review & Editing.

Declaration of Competing Interest

The authors declare that they have no known competing financial interests or personal relationships that could have appeared to influence the work reported in this paper.

Acknowledgments

This work was supported by the innovative R&D project in Guangdong Province in China [2019ZT08G669] and the National Natural Science Foundation of China [Grant Number: 41775067]. The constructive comments and suggestions from the three anonymous reviewers and the editor have significantly improved the revised manuscript.

References

Abatzoglou, J.T., Williams, A.P., 2016. Impact of anthropogenic climate change on wildfire across western US forests. P. Natl. Acad. Sci. USA 113, 11770–11775.
Abatzoglou, J.T., et al., 2013. Diagnosing santa ana winds in Southern California with synoptic-scale analysis. Weather Forecast. 28, 704–710.
Balch, J.K., et al., 2017. Human-started wildfires expand the fire niche across the United States. P. Natl. Acad. Sci. USA 114, 2946–2951.
Balch, J.K., et al., 2018. Switching on the Big Burn of 2017. Fire 1, 17.
Bendix, J., Hartnett, J.J., 2018. Asynchronous lightning and Santa Ana winds highlight human role in southern California fire regimes. Environ. Res. Lett. 13, 074024.
Billmire, M., et al., 2014. Santa Ana winds and predictors of wildfire progression in southern California. Int. J. Wildland Fire 23, 1119–1129.
Brewer, M.J., Clements, C.B., 2020. The 2018 Camp fire: meteorological analysis using in situ observations and numerical simulations. Atmosphere-Basel 11.
Cao, Y., Fovell, R.G., 2016. Downslope windstorms of San Diego county. Part I: a case study. Mon. Weather Rev. **144**, 529–552.
Coen, J.L., et al., 2020. Computational modeling of extreme wildland fire events: a synthesis of scientific understanding with applications to forecasting, land management, and firefighter safety. J. Comput. Sci. **45**, 101152.
Crockett, J.L., Westerling, A.L., 2018. Greater temperature and precipitation extremes intensify Western U.S. droughts, wildfire severity, and sierra nevada tree mortality. J. Clim. **31**, 341–354.
Dee, D.P., et al., 2011. The ERA-Interim reanalysis: configuration and performance of the data assimilation system. Q. J. Roy. Meteor. Soc. 137, 553–597.
Dennison, P.E., et al., 2014. Large wildfire trends in the western United States, 1984-2011. Geophys. Res. Lett. 41, 2928–2933.
Du, J., et al., 2013. Ensemble anomaly forecasting approach to predicting extreme weather demonstrated by extremely heavy rain event in Beijing. Chin. J. Atmos. Sci. 38, 685–699.
Giannaros, T.M., et al., 2020. Performance evaluation of an operational rapid response fire spread forecasting system in the southeast Mediterranean (Greece). Atmosphere-Basel **11**.
Goss, M., et al., 2020. Climate change is increasing the likelihood of extreme autumn wildfire conditions across California. Environ. Res. Lett. 15, 094016.
Graham, R.A., Grumm, R.H., 2010. Utilizing normalized anomalies to assess synoptic-scale weather events in the Western United States. Weather Forecast. 25, 428–445.
Grumm, R.H., 2011. The central European and Russian heat event of July-August 2010. B. Am. Meteorol. Soc. 92, 1285–1296.
Grumm, R.H., Hart, R., 2001. Standardized anomalies applied to significant cold season weather events: preliminary findings. Weather Forecast. 16, 736–754.
Guzman-Morales, J., et al., 2016. Santa Ana Winds of Southern California: their climatology, extremes, and behavior spanning six and a half decades. Geophys. Res. Lett. 43, 2827–2834.
Hart, R.E., Grumm, R.H., 2001. Using normalized climatological anomalies to rank synoptic-scale events objectively. Mon. Weather Rev. 129, 2426–2442.
Hughes, M., Hall, A., 2010. Local and synoptic mechanisms causing Southern California's Santa Ana winds. Clim. Dyn. 34, 847–857.
Hughes, M., et al., 2009. Anthropogenic Reductions of Santa Ana Winds. California Climate Change Center.
Jiang, N., et al., 2016. A comprehensive approach from the raw and normalized anomalies to the analysis and prediction of the Beijing extreme rainfall on July 21, 2012. Nat. Hazards 84, 1551–1567.
Jin, Y.F., et al., 2014. Contrasting controls on wildland fires in Southern California during periods with and without Santa Ana winds. J. Geophys. Res-Biogeo 119, 432–450.
Jin, Y.F., et al., 2015. Identification of two distinct fire regimes in Southern California: implications for economic impact and future change. Environ. Res. Lett. **10**.
Junker, N.W., et al., 2008. Use of Normalized Anomaly Fields to Anticipate Extreme Rainfall in the Mountains of Northern California. Weather Forecast 23, 336–356.
Junker, N.W., et al., 2009. Assessing the potential for rare precipitation events with standardized anomalies and ensemble guidance at the hydrometeorological prediction center. B. Am. Meteorol. Soc. 90, 445–453.
Keeley, J.E., Syphard, A.D., 2016. Climate change and future fire regimes: examples from California. Geosciences **6**.
Khorshidi, M.S., et al., 2020. Increasing concurrence of wildfire drivers tripled megafire critical danger days in Southern California between1982 and 2018. Environ. Res. Lett. 15, 104002.
Kolden, C.A., Abatzoglou, J.T., 2018. Spatial distribution of wildfires ignited under katabatic versus non-katabatic winds in Mediterranean Southern California USA. Fire 1, 19.
Mao, Y., et al., 2015. Is climate change implicated in the 2013-2014 California drought? A hydrologic perspective. Geophys. Res. Lett. 42, 2805–2813.
Marlon, J.R., et al., 2012. Long-term perspective on wildfires in the western USA. Proc. Natl. Acad. Sci. U. S. A. 109, E535–E543.
Mass, C.F., Ovens, D., 2019. The Northern California wildfires of 8-9 October 2017: the role of a major downslope wind event. B. Am. Meteorol. Soc. 100, 235–256.
Menne, M.J., et al., 2012a. An overview of the global historical climatology network-daily database. J. Atmos. Ocean. Technol. 29, 897–910.
Menne, M.J., Durre, Imke, Korzeniewski, Bryant, McNeal, Shelley, Thomas, Kristy, Yin, Xungang, Anthony, Steven, Ray, Ron, Vose, Russell S., Gleason, Byron E., Houston, Tamara G., 2012b. Global Historical Climatology Network - Daily (GHCN-Daily). NOAA National Climatic Data.
Miller, N.L., Schlegel, N.J., 2006. Climate change projected fire weather sensitivity: California Santa Ana wind occurrence. Geophys. Res. Lett. **33**.
Miller, J.D., et al., 2012. Trends and causes of severity, size, and number of fires in northwestern California, USA. Ecol. Appl. 22, 184–203.
Minnich, R.A., Chou, Y.H., 1997. Wildland fire patch dynamics in the chaparral of southern California and northern Baja California. Int. J. Wildland Fire 7, 221–248.
Moritz, M.A., et al., 2010. Spatial variation in extreme winds predicts large wildfire locations in chaparral ecosystems. Geophys. Res. Lett. **37**.
Nauslar, N.J., et al., 2018. The 2017 North Bay and Southern California fires: a case study. Fire 1, 18.
Peterson, D.A., et al., 2015. THE 2013 RIM FIRE implications for predicting extreme fire spread, pyroconvection, and smoke emissions. B. Am. Meteorol. Soc. 96, 229–247.
Qian, W.H., 2017. Temporal Climatology and Anomalous Weather Analysis. Springer Atmospheric Sciences, Singapore.
Qian, W.H., et al., 2014. A generalized beta-advection model to improve unusual typhoon track prediction by decomposing total flow into climatic and anomalous flows. J. Geophys. Res.-Atmos. 119, 1097–1117.
Qian, W., et al., 2021a. Anomaly-based synoptic analysis and model product application for 2020 summer southern China rainfall events. Atmos. Res. 258, 105631.
Qian, W.H., et al., 2021b. A review: anomaly-based versus full-field-based weather analysis and forecasting. B. Am. Meteorol. Soc. 102, E849–E870.
Rager, J.E., et al., 2021. Mixtures modeling identifies chemical inducers versus repressors of toxicity associated with wildfire smoke. Sci. Total Environ. 775, 145759.
Robeson, S.M., 2015. Revisiting the recent California drought as an extreme value. Geophys. Res. Lett. 42, 6771–6779.
Rundel, P.W., 2018. California chaparral and its global significance. In: Underwood, E.C., Safford, H.D., Molinari, N.A., Keeley, J.E. (Eds.), Valuing Chaparral: Ecological, Socio-Economic, and Management Perspectives. Springer International Publishing, Cham, pp. 9–14.
Santos, A.C.D., et al., 2021. Managing fires in a changing world: fuel and weather determine fire behavior and safety in the neotropical savannas. J. Environ. Manag. 289, 112508.
Silveira, S., et al., 2021. Chronic mental health sequelae of climate change extremes: a case study of the deadliest Californian wildfire. Int. J. Environ. Res. Public Health **18**.
Swain, D.L., 2021. A shorter, sharper rainy season amplifies California wildfire risk. Geophys. Res. Lett. **48** e2021GL092843.

Syphard, A.D., et al., 2007. Human influence on California fire regimes. Ecol. Appl. 17, 1388–1402.
Thorne, J.H., et al., 2017. The impact of climate change uncertainty on California's vegetation and adaptation management. Ecosphere **8**.
Westerling, A.L., et al., 2004. Climate, Santa Ana Winds and autumn wildfires in southern California. Eos 85, 289.
Westerling, A.L., et al., 2011. Climate change and growth scenarios for California wildfire. Clim. Chang. 109, 445–463.
Williams, A.P., et al., 2015. Contribution of anthropogenic warming to California drought during 2012-2014. Geophys. Res. Lett. 42, 6819–6828.
Williams, A.P., et al., 2019. Observed impacts of anthropogenic climate change on wildfire in California. Earths Future 7, 892–910.
Worsnop, R.P., et al., 2020. Extended-range probabilistic fire-weather forecasting based on ensemble model output statistics and ensemble copula coupling. Mon. Weather Rev. 148, 499–521.
Xiang, J., et al., 2021. Field measurements of PM2.5 infiltration factor and portable air cleaner effectiveness during wildfire episodes in US residences. Sci. Total Environ. **773**, 145642.